Unsteady Response of an Axial Flow Compressor to Planar Temperature Transients

D. K. Das*
SUNY College of Technology, Utica, New York
A. Trippi†
Cranfield Institute of Technology, Cranfield, United Kingdom
and
R. E. Peacock‡
Naval Postgraduate School, Monterey, California

A spatially one-dimensional, time-dependent mathematical model to analyze the effects of pressure and temperature fluctuations on the dynamic response of a compression system is presented. The model accounts for the compressor unsteady response, variation of compressor efficiency with the flow coefficient, and the variation of air specific heats with temperature. The continuity, momentum, and energy equations are written for the inlet, compressor, and outlet duct, together with a first-order relaxation equation describing the unsteady response of the compressor. The resulting system of hyperbolic partial differential equations is solved by the method of characteristics. The model is used to simulate the convection of planar temperature fluctuations (entropy waves) into a compression system.

Nomenclature

A = cross-sectional area
A_t = throttle cross-sectional area
a = sonic speed
a_a = reference sonic speed [see Eq. (14)]
C_x = axial velocity
C_{xB} = air bleeding flow axial velocity
C'_{xB} = see Eq. (5)
C_p = specific heat at constant pressure
C_v = specific heat at constant volume
D = hydraulic diameter
e_0 = total energy
f = friction coefficient
F_a = distribution of axial forces.
h = enthalpy
$\dot{h}$ = dh/dT [see Eq. (2)]
h_0 = total enthalpy
h_{0B} = air bleeding flow total enthalpy
h'_{0B} = see Eq. (5)
$\dot{h}_a$ = $\dot{h}(a_a)$
ℓ = stage length
$\dot{m}_1, \dot{m}_2$ = mass flow rate at plenum chamber inlet and outlet, respectively
p = static pressure
P_a = reference pressure
P_p = plenum chamber pressure
Q = heat transfer per unit length, per unit time
R = gas constant
t = time
T = static temperature
T_{0I} = total temperature at plenum chamber inlet
T_p = plenum chamber temperature
V_p = plenum chamber volume
W = work transfer per unit length, per unit time
x = axial coordinate
γ = specific heats ratio
$\dot{\gamma}$ = $d\gamma/da$ [see Eq. (3)]
$\dot{\gamma}_a$ = $\dot{\gamma}(a_a)$
$\Gamma_1, \Gamma_2, \Gamma_3$ = see Eq. (7)
μ = throttle flow factor
ρ = density
ψ = air bleeding mass flow rate
ψ_{AM} = air bleeding flow axial momentum
ψ_E = air bleeding flow total enthalpy

Introduction

IN modern aircraft, flow instabilities form an important aspect of airframe/engine integration. These instabilities may be due to flow perturbations generated by such phenomena as intake buzz, hot gas ingestion, and sharp maneuvers. These are characterized by large planar pressure and/or temperature fluctuations. As a consequence, the compressor is forced away from its steady operating point and, depending upon its dynamic response, eventually, there may be a complete breakdown in the flow leading to surge. This not only imposes drastic limitations on the performance and operational limits of the propulsion system, but also may lead to severe structural damages.

The occurrence of flow instabilities caused by fast temperature transients is particularly important in the design and development of military aircraft, the engines of which are subject to steep inlet temperature changes as a consequence of missile and gun firing, steam ingestion, and VTOL operations.[1-4] In civil aircraft, hot gasses may be ingested into the engines during thrust reversal operations. The experimental data available in the literature on the effects of temperature transients on engine response are considerably fewer than those available for the case of pressure per-

Received June 16, 1982; presented as Paper 82-1266 at the AIAA 18th Joint Propulsion Conference, Cleveland, Ohio, June 21-23, 1982; revision received June 30, 1984.

*Associate Professor, Division of Engineering Technology.
†Research Student, The School of Mechanical Engineering.
‡Lately NAVAIR Professor of Aeronautics.

turbations. Experimental results on the dynamic response of turbojet and turbofan engines to inlet total temperature ramps may be found in Refs. 3-10. These results have brought out the basic physical phenomena governing the engine tolerance to sharp inlet temperature rises and the qualitative description provided therein regarding the events leading to compressor surge may be considered valid for multistage compressors in general.

The mathematical modeling of the propulsion system accounting for the abovementioned phenomena is made difficult by the complexity of the dynamic response of the various components of the system. In recent years, various attempts[11-14] have been made to simulate such a system mathematically. The importance of these models can be summarized as follows:

1) they provide a better understanding of the basic physical principles governing the dynamic response of the propulsion system to flow unsteadiness, and

2) they enable the airframe and engine designers to define the influence of the various design parameters on the dynamic behavior of the airframe/engine system, its performance, and surge tolerance.

This paper presents a model in which the propulsion system consists of a series of one-dimensional ducts, each of them representing one element of the system, i.e., intake, compressor, combustion chamber, turbine, nozzle, and exhaust. The flow within each duct is assumed spatially one-dimensional and unsteady. Time-dependent distributions are introduced to simulate friction and blade forces, heat and work transfer, and air bleeding. The governing equations have been introduced by Rannie[11] and Horlock and Daneshyar.[12] Pursuing a similar approach, two different models have been developed at the Cranfield Institute of Technology over the past few years as part of a theoretical and experimental research program on unsteady flow in axial flow compressors.[13,15-17] The first model (the actuator disk model) assumes the flow to be homentropic and the work done by each stage is added over an infintesimally short axial distance. The second model (the continuous flow model) accounts for the presence of entropy waves (nonhomentropic flow) and the energy transfer within the compressor is distributed continuously over a finite distance. In both cases the method of characteristics is used to solve the governing system of hyperbolic partial differential equations.

The two models have been used extensively to simulate the dynamic response of a compression system with pulsed pressure fluctuations at the inlet. Comparison between theoretical and experimental results and the application of the continuous flow model to the convection of entropy waves into the intake duct suggested some modifications to the continuous flow model in order to improve the accuracy of the mathematical model and to speed up the numerical solution of the governing equations.

Mathematical simulation of the propagation of entropy waves is rather expensive in terms of computing time. In fact, unlike pressure waves which travel at sonic speed with reference to the flow, entropy waves travel at the flow velocity and, therefore, a longer time has to be simulated to allow for any flow instability to develop fully. Furthermore, the Courant-Friedrichs-Lewy (CFL) condition used for the numerical solution of the governing system of hyperbolic partial differential equations requires the time step to be decreased as the sonic speed increases. Therefore, a higher number of time steps is required to simulate the same time interval compared to the case of pressure fluctuations only.

In the present form of the model, a better description of the compressor has been achieved by accounting for the variation of the compressor efficiency with the flow coefficient C_x/U and adopting a first-order relaxation equation to model the compressor dynamic response as proposed by several authors.[18-22] The working fluid has been assumed to be a homogeneous thermally perfect gas in order to account for the variation of the specific heats with temperature. This is significant in the simulation of the combustion chamber, the multistage compressor, as well as large-amplitude temperature fluctuations.

All of these modifications are intended to make the existing model better matched to analyze situations encountered during the operative lift of a real aircraft engine with the ingestion of hot gases, both in civil (thrust reversal on landing) and military (thrust reversal, VTOL operations, and armament firing) applications. The improvement to the combustion chamber simulation and the introduction into the basic equations of terms representing time-dependent mass removal or additional (such as interstage or compressor discharge air bleed) enable the model to analyze the response of the propulsion system to the ingestion of hot gases and the effects of possible remedials such as fuel derichment and air bleeding.

The model has been applied to a three-stage compressor and the results show the influence of the magnitude and the rate of change of temperature on the stability limit of the compression system.

Table 1 Compressor geometry

No. of stages	3
Tip diameter (stage 1)	0.51 m
Hub/tip ratio (stage 1)	0.67
Design rotational speed	150 rev/s
Design mass flow	18.14 kg/s
Rotational speed used in this investigation	133.33 rev/s

Basic Equation of the Model

The compression system is modeled as a series of bladed and unbladed ducts wherein flow is assumed to be spacewise one-dimensional depending only on the axial coordinate x and time t: Therefore, planar disturbances only are simulated. Within each duct, proper time-dependent distributions are introduced in order to simulate friction and blade forces, heat transfer, and air bleeding, as shown schematically in Fig. 1. The friction and blade forces are represented by a distribution of body forces which, within the compressor, are computed by splitting each stage into a number of infinitesimally small stages in series. The radial and tangential components of the velocity and force vectors are assumed to be negligible when compared with the axial components. The flow is also assumed to return to the axial direction after each of the infinitesimally small stages.

The fluid is considered to be a homogeneous thermally perfect gas accounting for specific heat variations with temperature so that the following thermodynamic relationships hold:

$$C_p = C_p(T) \tag{1a}$$

$$C_v = C_v(T) \tag{1b}$$

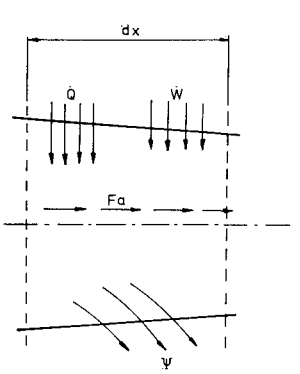

Fig. 1 Control volume.

and

$$\dot{h}=\frac{\mathrm{d}h}{\mathrm{d}a}=\frac{C_p}{\mathrm{d}a/\mathrm{d}T} \tag{2}$$

$$\dot{\gamma}=\frac{\mathrm{d}\gamma}{\mathrm{d}a}=\frac{2\gamma}{a}-\frac{\dot{h}}{a^2}\gamma(\gamma-1) \tag{3}$$

The continuity, axial momentum, and energy equations can be written both for the bladed and unbladed ducts.
Continuity:

$$\frac{\partial(\rho A)}{\partial t}+\frac{\partial(\rho A C_x)}{\partial x}+\psi=0 \tag{4a}$$

Axial momentum:

$$\frac{\partial(\rho A C_x 2)}{\partial x}+\frac{\partial(\rho A C_x)}{\partial t}+\psi_{AM}=F_a-A\frac{\partial P}{\partial x} \tag{4b}$$

Energy:

$$\frac{\partial(\rho A C_x h_0)}{\partial x}+\frac{\partial(\rho A e_0)}{\partial t}+\psi_E=\dot{Q}+\dot{W} \tag{4c}$$

Let

$$\psi_{AM}=\psi C_{xB}=\psi(C_x+C'_{xB}) \tag{5a}$$

$$\psi_E=\psi h_{0B}=\psi(h_0+h'_{0B}) \tag{5b}$$

By substitution of Eqs. (1-3) and (5) into Eqs. (4) we obtain

$$\left(2-a\frac{\dot{\gamma}}{\gamma}\right)\frac{\partial a}{\partial t}+C_x\left(2-a\frac{\dot{\gamma}}{\gamma}\right)\frac{\partial a}{\partial x}$$
$$-a\frac{\partial C_x}{\partial x}-\frac{a}{P}\frac{\partial P}{\partial t}-\frac{C_x a}{P}\frac{\partial P}{\partial x}=2\Gamma_1 \tag{6a}$$

$$C_x\frac{\partial C_x}{\partial x}+\frac{\partial C_x}{\partial t}+\frac{a^2}{\gamma P}\frac{\partial P}{\partial x}=\Gamma_2 \tag{6b}$$

$$\dot{h}\frac{\partial t}{\partial t}+C_x\dot{h}\frac{\partial a}{\partial x}+C_x\frac{\partial C_x}{\partial t}+C_x^2\frac{\partial C_x}{\partial x}-\frac{a^2}{p\gamma}\frac{\partial P}{\partial t}=\Gamma_3 \tag{6c}$$

where

$$\Gamma_1=\frac{1}{2}\left(\frac{aC_x}{A}\frac{\mathrm{d}A}{\mathrm{d}x}+\psi\frac{a^3}{PA\gamma}\right) \tag{7a}$$

$$\Gamma_2=\frac{F_a-\psi C'_{xB}}{\rho A} \tag{7b}$$

$$\Gamma_3=\frac{a_2}{PA_\gamma}\left(\dot{Q}+\dot{W}-\psi h'_{0B}\right) \tag{7c}$$

Equations (6) form a system of three partial differential equations where x and t are the independent variables and a, P, and C_x are the dependent variables.

The axial forces and the work term in Eqs. (7) can be computed for the unbladed ducts from

$$\dot{W}=0 \tag{8a}$$

$$F_a=-\frac{\rho C_x 2}{2}\frac{4f}{D}A \tag{8b}$$

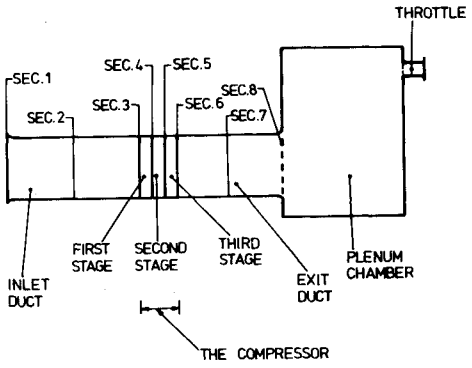

Fig. 2 Compression system layout.

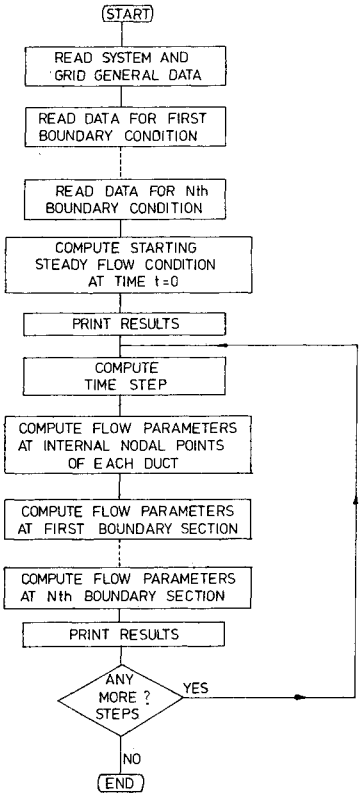

Fig. 3 Computer program flowchart.

Within a bladed duct the computation of these terms becomes more complicated. The dynamic response of a compressor is, in fact, deeply affected by the flow unsteadiness and its behavior can be considerably different from that for steady flow. In recent years different methods have been proposed to reproduce mathematically the compressor response to perturbations at its inlet. One way of simulating such a response is to approximate the blade row/airflow system in each stage to a first-order linear system whose dynamic behavior is represented by the expression

$$\tau\frac{\mathrm{d}X}{\mathrm{d}t}=X_{ss}-X \tag{9}$$

where τ is the time lag constant, X the effective value of the axial forces and work supplied to the system by the compressor, and $X_{ss}=X$ in steady flow.

The time lag constant τ depends on the compressor characteristics and the operating point. Usually three different regions are defined in the compressor characteristic

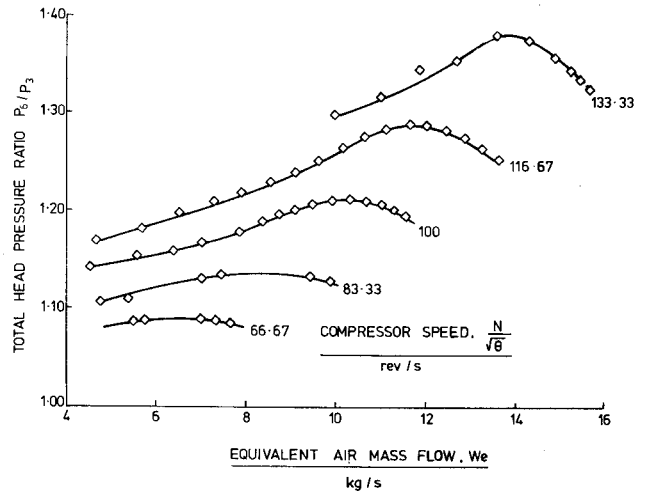

Fig. 4 Overall characteristics of the compressor.

map where a different value of the time constant τ may be defined—unstalled region, rotating stall inception region, or rotating stall region. Only limited data are presently available on the effects of flow fluctuations on the compressor response.

The steady-state term X_{ss} in Eq. (9) can be computed by splitting each stage into an infinite number of small stages and neglecting changes in axial velocity across the stage. From the momentum and energy equations in steady flow, together with the definition of polytropic efficiency, we obtain

$$\left(\frac{F_a}{\rho A}\right)_{ss} = \eta_p \frac{\Delta h}{\ell} \tag{10a}$$

$$\left(\frac{\dot{W}}{\rho A}\right)_{ss} = C_x \frac{\Delta h}{\ell} \tag{10b}$$

The terms ψ, C'_{xB}, and h'_{0B} depend on the geometry and dynamic response of the air bleeding system. They are assumed to be known functions of C_x, a, and P, but not of their derivatives. The same holds for Q.

The problem described thus far is classified as an initial boundary value problem for which boundary conditions are to be given (in the x-t plane) at each point along the x axis at $t=0$ and along the time axis at the inlet and outlet sections of the system. The initial flow condition along the x axis at the time $t=0$ can be computed assuming any perturbation to start from a steady-state flow condition. The number and type of flow parameters to be assigned at each end depend on the physical configuration of the system under consideration and the flow characteristics. For the layout shown in Fig. 2, it is assumed that the total pressure and total temperature are given at the inlet as functions of time. The static pressure is given as the boundary condition at the outlet section computed according to the following equations:

$$\frac{dp_p}{dt} = \left(\dot{m}_1 T_{01} - \dot{m}_2 T_p\right)\frac{C_p(\gamma-1)}{V_p} \tag{11a}$$

$$\frac{dT_p}{dt} = \frac{1}{P_p}\left[\frac{RT_p^2}{V_p}(\dot{m}_2 - \dot{m}_1) + T_p\frac{dP}{dt}\right] \tag{11b}$$

$$\dot{m}_2 = (P_p A_t/\sqrt{T_p})\,\mu \tag{11c}$$

which describe the dynamic response of the plenum chamber downstream of the compressor.

Method of Solution

Equations (6) form a system of hyperbolic partial differential equations for which a set of three characteristic and compatibility equations can be written.

First characteristic line (path line)

$$\lambda = \frac{dx}{dt} = C_x \tag{12a}$$

$$da_a = \left(\frac{a_a}{a}\right)^2 \frac{\gamma}{\gamma_a}\frac{1}{\dot{h}_a}(\Gamma_3 - \Gamma_2 C_x)\,dt \tag{12b}$$

Second and third characteristic lines (right- and left-going characteristic lines)

$$\lambda = \frac{dx}{dt} = C_x \pm a \tag{13a}$$

$$\left[\frac{\dot{h}\gamma}{a} + a\frac{\dot{\gamma}}{\gamma} - 2\right]da \pm dC_x = \frac{a}{a_a^2}\frac{\gamma a}{\gamma}\dot{h}_a da_a + \left\{-2\Gamma_1 + \frac{\Gamma_2}{a}\left[C_x(1-\gamma) \pm a\right] + \Gamma_3\frac{(\gamma-1)}{a}\right\}dt \tag{13b}$$

In these equations the dependent variable P has been replaced by the "reference sonic speed" defined (for a given reference pressure P_a) by

$$\ell n\frac{P}{P_a} = \int_{a_a}^{a}\frac{\dot{h}\gamma}{a^2}\,da \tag{14}$$

Equations (12) and (13) are integrated numerically by a rectangular grid in the x-t plane. The ordinary differential equation (9) is solved numerically at each time step and the result is used in computing the axial forces and the work term in Γ_2 and Γ_3. Analogously, Eqs. (11) are solved numerically at each time step and the static pressure so computed is used as the assigned flow parameter at the system outlet.

In previous models[12,13] based on the method of characteristics, a polytropic relationship has been used instead of the axial momentum equation for the bladed duct. The present form of the model allows the same set of equations to be used both for the bladed and unbladed ducts and, therefore, simplifies the program coding. Moreover, the computation of the direction equations for the wave characteristics does not require any iterative method as do the abovementioned methods for the case of nonhomentropic flow.

The software for the solution of the governing equations has been developed as a package of subroutines by which it is possible to analyze other layouts different from and more complicated than that shown in Fig. 2 (such as two compressors in series or a complete engine including a turbine and a nozzle) by stacking the available routines. As shown in Fig. 3, the software is built up around a main subroutine which computes the flow parameters for the bladed and unbladed ducts at each nodal point except the first and the last. Besides this subroutine, a series of different subroutines has been developed for different boundary conditions between two or more ducts and at the inlet and outlet of the system. These subroutines compute the flow parameters at the first and last nodal points of each duct.

Example of Application

As a representative example of application, the mathematical model described in the previous paragraphs has been applied to simulate the response of a research compressor used in a research program on unsteady flow in axial flow compressors[15-17] to temperature transients.

The general layout of this research facility is shown schematically in Fig. 2. The compressor consists of the first three stages of a Proteus Mark II aircraft compressor. Its overall characteristic curves are shown in Figs. 4 and 5 and the leading particulars are given in Table 1.

As represented in Fig. 4, the compressor under consideration is characterized by rather flat pressure ratio/mass flow curves (especially at low corrected rotational speed). As the peak is passed in reducing the mass flow rate, the pressure ratio reduces progressively. Here the effect of the rotating stall is progressive rather than impulsive, resulting in a continuous deterioration of the compressor performance. Similar features are shown by each characteristic of the stage. On the positive slope region of the characteristic map, the pressure ratio of the first two stages decreases very slowly with an abrupt drop only at very small values of the mass flow rate, whereas, for the third stage, the characteristic curve has a continuously falling drop without any abrupt fall.

A parametric analysis was carried out for the time constant τ in Eq. (9) with values ranging from 0 to 0.003 s in order to assess the influence of the compressor dynamic response on the system behavior. No substantial difference resulted in the response of the compressor under consideration and, hence, all of the results shown herein are relevant to the case $\tau = 0$, i.e., the case of steady-state compressor response. Given the particular characteristic curves of the compressor simulated, this should not lead to any general conclusion about the importance of the time constant τ as one of the driving parameters in the dynamic response of an axial flow compressor during temperature transients.

The simulation was carried out for five different nonterminating temperature ramps imposed at the system inlet (1000, 2000, 3000, 4000, and 5000 K/s) and data for 3000 and 5000 K/s are presented in Figs. 6-9 inclusive. The remaining boundary conditions, total pressure at the inlet of the intake duct, and static pressure at the outlet of the exhaust duct were held constant. The latter condition corresponds to the case of a plenum chamber of infinite volume fitted downstream of the compressor as suggested by previous experimental results gained from the same test facility. The computation was stopped when negative velocity was computed within the compressor since no realistic data were available for reverse flow and such flow conditions may be considered indicative of the surge onset in the compression system.

The system response for every temperature ramp is somewhat similar, except that the progression of events became more rapid with increased temperature ramp. Therefore, reference is made only to the 3000 K/s temperature ramp case (see Figs. 6 and 7).

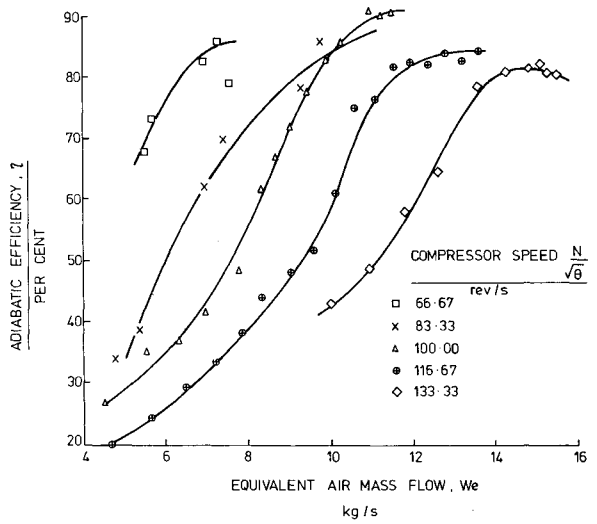

Fig. 5 Variation of adiabatic efficiency with equivalent mass flow.

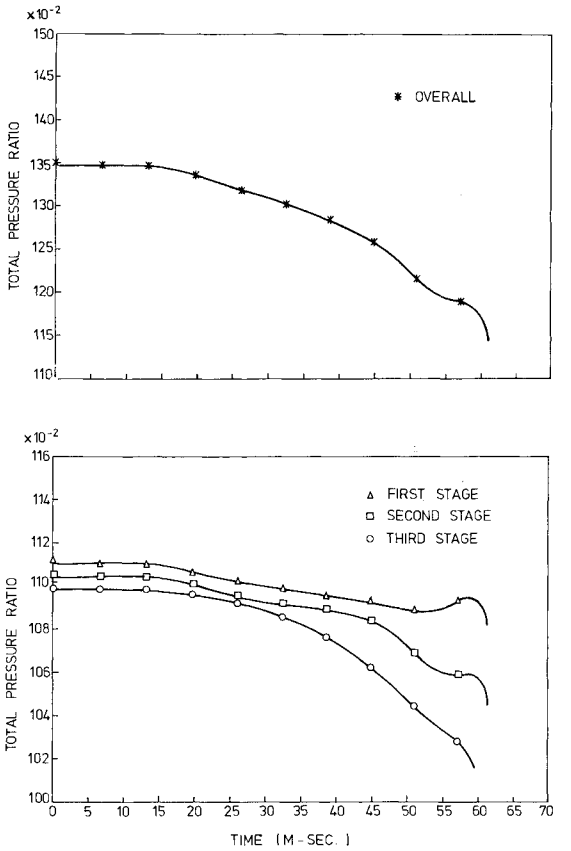

Fig. 6 Stage and overall total pressure ratio variation, temperature ramp 3000 K/s.

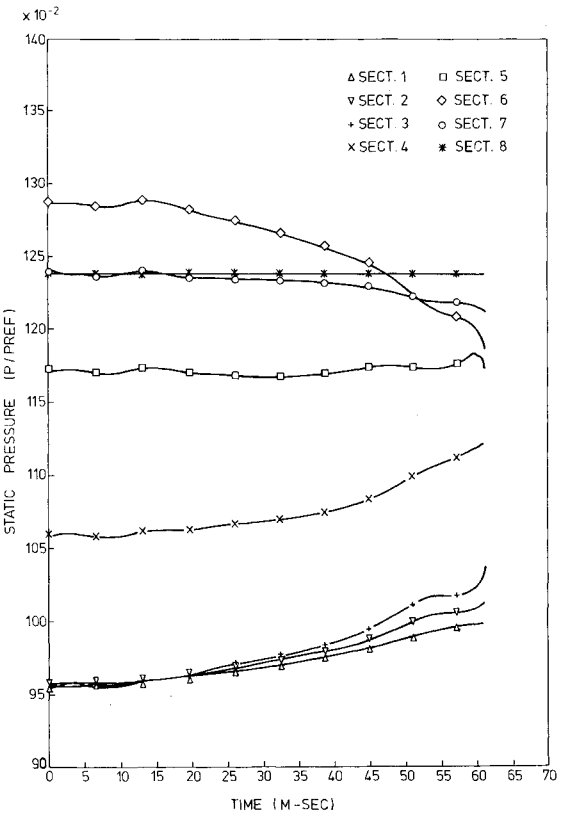

Fig. 7 Static pressure variation, temperature ramp 3000 K/s.

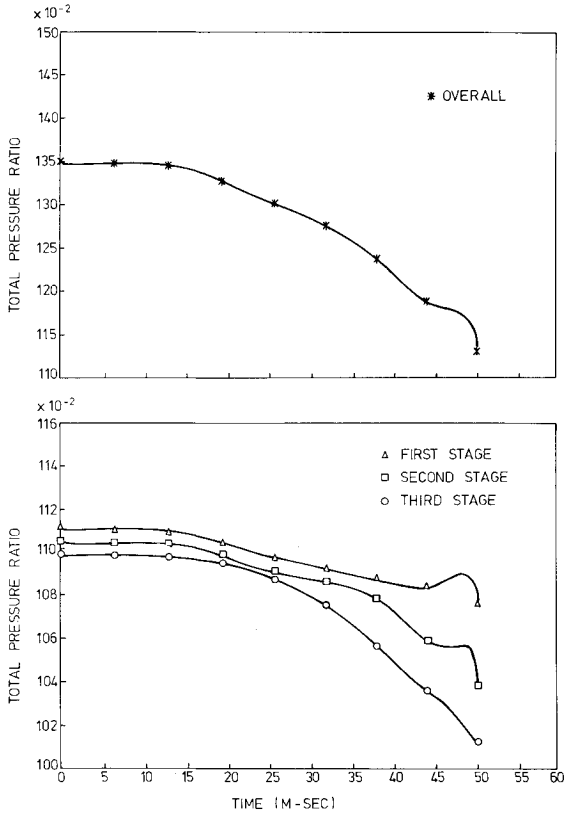

Fig. 8 Stage and overall total pressure ratio variation, temperature ramp 5000 K/s.

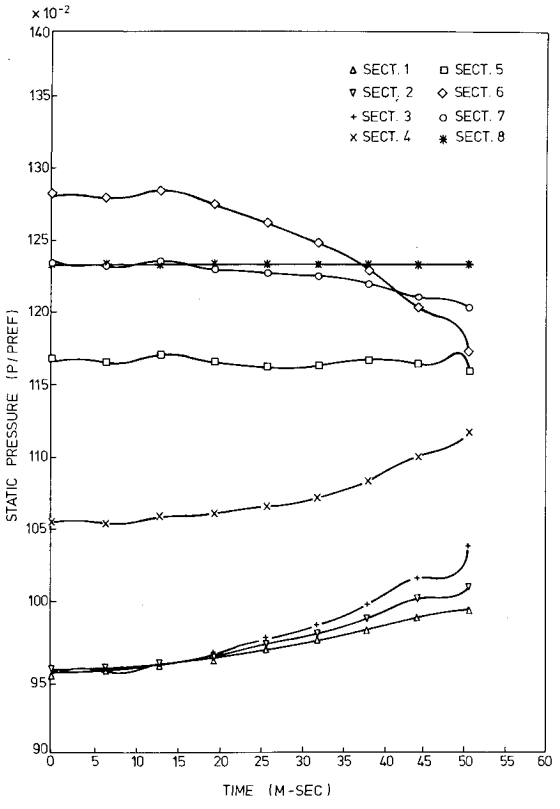

Fig. 9 Static pressure variation, temperature ramp 5000 K/s.

Over the period of the calculation the associated pressure wave generated by the existence of the temperature pulsation passed, with its reflections, several times through the system yielding the nonlinear, but continuous, static pressure rise toward the front of the system (Secs. 1-4 of Fig. 7). The fairly continuous fall of static pressure at the compressor exit was a consequence of the dominating effect, at the plane, of the generally reduced work through the compressor as the operating point moved to a low C_x/U condition. At the second stage exit plane (Sec. 5) these two effects tended to cancel. The effect upon stage pressure ratio was a stage-by-stage reduction after about 13 ms resulting in a progressive reduction in overall pressure ratio before system destabilization.

The mechanism leading to system destabilization may be explained as follows. After about 45 ms a more rapid deterioration at the second-stage pressure ratio was accompanied by a sharp rise in the entry static pressure. This increased the first-stage pressure ratio forcing it toward instability, followed by a sharp fall in pressure ratio as the operating point moved to the positive slope portion of the characteristic. This led to a breakdown of the flow in both the first and second stages indicated by the sharp terminating rise in static pressure at first-stage entry (Sec. 3) and an accompanying fall in the static pressure at second-stage exit (Sec. 5). As a consequence of the flow blockage at the first two stages, a hammershock pressure wave propagated upstream and a rarefaction wave downstream of the compressor. It is noted that the static pressure rise at the second-stage exit (Sec. 5) resembles that mentioned in Ref. 2 as an indicator of the occurrence of surge in the low-pressure compressor of two turbofan engines during a series of steam ingestion tests.

Figure 10 indicates the total temperature achieved at compressor inlet (Sec. 3) at the point of surge for the range of temperature ramp employed. The relationship is almost linear, showing that, due to the system response rate, a higher level was encountered with more rapid temperature ramps.

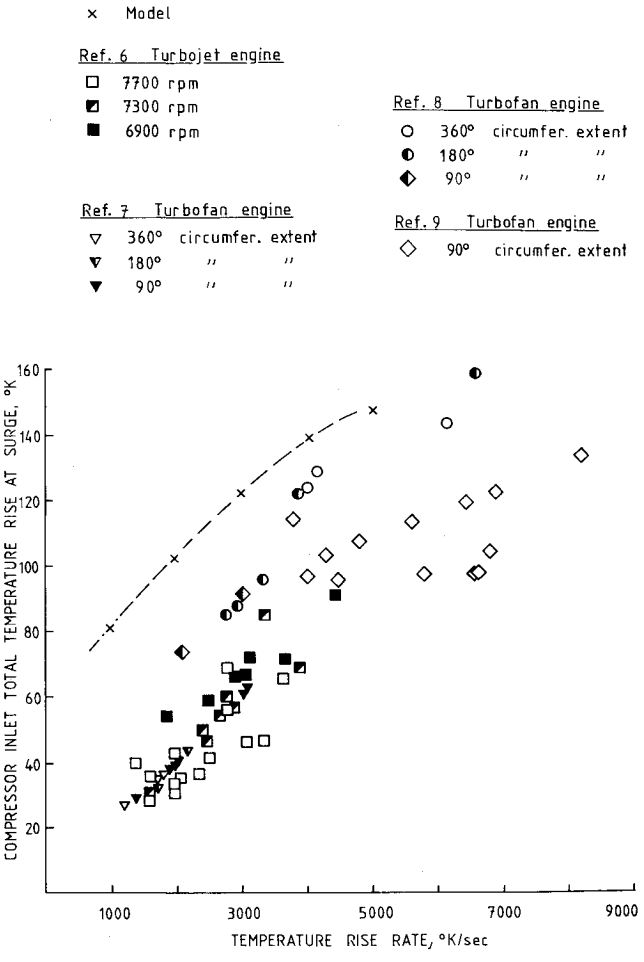

Fig. 10 Compressor inlet total temperature rise at surge.

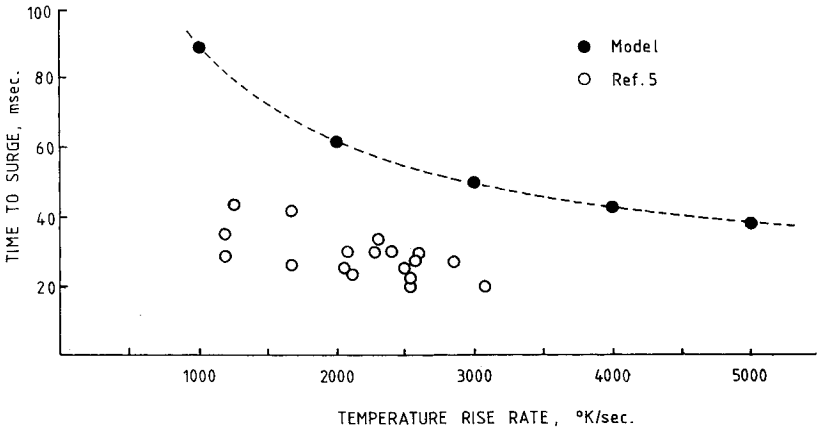

Fig. 11 Time to surge.

The time to surge from temperature ramp inception is indicated in Fig. 11. The nonlinear relationship indicates that while surge is more quickly encountered there is an irreducible time associated with the wave transit time through the system.

Discussion

Possibly because of the difficulty in establishing a well-controlled experiment, very few data are currently available on the effect of the ingestion of planar entropy waves by a compressor embedded in ducting. From those which are known, there is the suggestion of a strong dependence upon the shape of the compressor characteristics. The sequence of events described herein hold for a compressor characteristic that is continuous at the instability line. It is not likely that they would represent the reaction of a system that has a discontinuity at destabilization. The calculated system reaction up to the instability point is probably typical for any compressor/duct system.

In this regard, it may be noted that the flow phenomena leading to surge as described in the model exhibit a close similarity to those determined experimentally as reported in Refs. 2, 5, 6, 8, and 9. In these tests the compressor stages moved during the temperature transients along an operating line of nearly constant pressure ratio. This phenomenon was not reproduced by the model. The discrepancy may be attributed to the difference in the shapes of the stage characteristic curves and the higher surge tolerance of the compressor simulated. This results in a longer time to surge from the temperature distortion inception, as confirmed by the data in Figs. 10 and 11. Also, it is evident from these data, that the results obtained from the model follow a trend similar to that of the experimental data found in the literature.

However, there are no experimental results available to compare directly with the analytical data presented and, while these data cannot be regarded as universal in their application, it is thought that the model is a useful tool in reaching a better understanding of the mechanism leading to system destabilization during a temperature transient and it is capable of reproducing the physical phenomena involved.

Conclusions

A mathematical model is proposed for the simulation of flow unsteadiness within a compression system. The model is based on the solution of the continuity, momentum, and energy equations by the method of characteristics. The application to the case of temperature ramps imposed at the system inlet proved that the model is capable of modeling the propagation of pressure and temperature waves. Very few data are available at present on the effects of the ingestion of planar entropy waves by a compressor embedded in a ducting; moreover, all of the available results suggest a strong dependence on the compressor characteristics. This makes impossible any comparison of the results shown in this paper with experimental data.

Nevertheless, the model was able to reproduce physical phenomena involved in destabilization and, hence, lead to a better understanding of the mechanism leading to the compressor surge during a temperature transient.

The governing equations and the computer software are developed in a rather general form allowing a simulation of layout and operational conditions different from those reported herein.

References

[1] Rich, W. A., "The Simulation of the Ingestion of Missile Exhaust by Turbojets," Paper presented at the National Conference on Environmental Effects on Aircrafts and Propulsion Systems, Trenton, N. J., 1971.

[2] Mallet, W. E. and Parcells, R. F., "Catapult Steam Ingestion Tests of Three Turbofan Engines in the A-7 Aircraft," Paper presented at the National Conference on Environmental Effects on Aircrafts and Propulsion Systems, Trenton, N. Y., 1971.

[3] Hercock, R. G. and Williams, D. D., "Aerodynamic Response," *Distortion Induced Engine Instability*, AGARD LS-72, Nov. 1972.

[4] Mabey, D. G. and Capps, D. S., "Blast from Moving Guns," *Journal of Aircraft*, Vol. 14, July 1977.

[5] Gabriel, D. S., Wallner, L. E., and Lubick, R. J., "Some Effects of Transients in Inlet Pressure and Temperature on Turbojet Engines," Institute of Aeronautical Sciences, Preprint 709, Jan. 1957.

[6] Wallner, L. E., Useller, J. W., and Saari, M. J., "A study of Temperature Transients at the Inlet of a Turbojet Engine," NACA RM E57C22, 1957.

[7] Rudey, R. A. and Antl, R. J., "The Effects of Inlet Temperature Distributions on the Performance of a Turbofan Engine Compressor System," AIAA 6th Propulsion Joint Specialist Conference, San Diego, Calif., June 1970.

[8] Abdelwahab, M., "Effects of Temperature Transients at Fan Inlet of a Turbofan Engine," NASA TP-1031, Sept. 1977.

[9] Abdelwahab, M., "Effects of Fan Inlet Temperature Disturbances on the Stability of a Turbofan Engine" NASA TM-82699, Dec. 1981.

[10] Hercock, R. G., "Effects of Intake Flow Distortions on Engine Stability," AGARD, PEP 60th Symposium on Engine Handling, Greece, Oct. 1981.

[11] Rannie, W. D., "The Response of an Axial Flow Compressor to Unsteady Disturbances" *Proceedings of a Workshop on Unsteady Flows in Jet Engines,* UARL, East Hartford, Conn. 1974.

[12] Horlock, J. H. and Daneshyar, H. "Turbomachinery Waves" *Aeronautical Quarterly*, Feb. 1977.

[13] Peacock, R. E. and Eralp, O. C., "Compressor Response to Spatially Repetitive and Nonrepetitive Transients," Israel Joint Gas Turbine Congress, Haifa, Israel, July 1979, Paper 79-GT-Isr-14.

[14] Chamblee, C. E., David, M. W., and Kimzey, W. F., "A Multi-Stage Axial Flow Compressor Mathematical Modeling Technique with Application to Two Current Turbofan Compression Systems," AIAA Paper, Pasadena, Calif., Jan. 1980.

[15] Peacock, R. E. and Das, D. K., "An Experimental Study of Pulsating Flow in a Three-Stage Axial Flow Compressor," Symposium on Nonsteady Fluid Dynamics, The Winter Annual Meeting of ASME, San Francisco, Calif., Dec. 1978.

[16]Peacock, R. E., Erlap, O. C., and Das, D. K., "Compressor Response to Pulsed Transients," AIAA/SAE/ASME 16th Joint Propulsion Conference, Hartford, Conn. June-July 1980.
[17]Peacock, R. E. and Das, D. K., "The Excitation of Compressor/Duct Systems," The Winter Annual Meeting of ASME, Washington, D. C., Nov. 1981.
[18]Takata, H., "Dynamic Performance of Blade Rows," NASA TT-F-11,838, July 1968.
[19]Takata, H., and Nogano, S., "Non-linear Analysis of Rotating Stall," ASME Paper 72-GT-3, 1972.
[20]Melick, H. C. and Simpkin, W. E., "A Unified Theory of Inlet/Engine Compatibility," AIAA/SAE 8th Joint Propulsion Specialist Conference, New Orleans, La., Nov.-Dec. 1972.
[21]Greitzer, E. M., "Surge and Rotating Stall in Axial Flow Compressors—Part 1: Theoretical Compression System Model", *Transactions of ASME, Journal of Engineering for Power*, Vol. 98, April 1976, pp. 190-198.
[22]Fabri, J. and Paulon, J., "Determination theorique et experimentale de al fonction de transport d'un compresseur," *La Recherche Aerospatiale*, No. 4, July-Aug. 1981, pp. 223-231.